The morphology of amputated human teeth and its relation to mechanical properties after restoration treatment

Jonas Gugger[a,b], Gabriel Krastl[a], Marius Huser[c], Hans Deyhle*[a,b], and Bert Müller[a,b]

[a]School of Dental Medicine, University of Basel, 4056 Basel, Switzerland;
[b]Biomaterials Science Center, University of Basel, 4031 Basel, Switzerland;
[c]ImageLab GmbH, 8400 Winterthur, Switzerland

ABSTRACT

The increased susceptibility to fracture of root canal- and post-treated teeth is less affected by alterations of the dentin structure, but seems to crucially depend on the loss of coronal tooth substance. The surface, available for adhesion of the composite material in the root canal and in the coronal part of the tooth, is assumed to be of key importance for the fracture resistance. Thus, an appropriate three-dimensional method should be identified to determine the adhesive surface with necessary precision. For this purpose, severely decayed teeth were simulated decapitating clinical crowns. After root canal filling and post space preparation, impressions of the root canal and the amputation surface were obtained using silicone. Micro computed tomography scans of these impressions were acquired. For one selected specimen, an additional high-resolution scan was recorded at a synchrotron radiation source. Software of ImageLab served for the extraction of the amputation interface, the post surface and the post volume from the tomography data, which have been finally correlated with the Young's modulus and the maximal load derived from mechanical tests. The morphological parameters show a realistic relationship to the mechanical tests performed after the restoration treatments and are consequently important for improving the dental skills.

Keywords: micro computed tomography, tooth morphology, root canal surface and volume, amputation interface, post treatment, Young's modulus, fracture resistance, morphology-mechanics relationship.

1. INTRODUCTION

After severe carious or traumatic decay, a root canal treatment is often necessary in order to preserve a compromised tooth. Intra-radicular posts are commonly used to provide support and retention for the coronal restoration [1]. Even though different treatment strategies and materials for restoration have been introduced during the last decades [2] prognosis is less favorable in root canal treated (RCT) compared to vital teeth [3]. In the recent literature there is general agreement, that the higher susceptibility to fracture of RCT teeth is less associated with alterations of the dentin structure as proposed in previous studies and seems to depend to a high extent on the loss of coronal tooth substance [2]. Reeh and co-workers revealed that cavity preparations with loss of the marginal ridge integrity significantly decrease the stiffness of the crown while endodontic procedures had only a small effect [4]. In a recent study, however, interferometric analysis was used for a more accurate assessment of the deformability of roots after endodontic measures, showing a considerable decrease in stability especially after post preparations [5].

The aim of the post-endodontic treatment is to re-stabilize the weakened crown and root. In general adhesive post-retained restorations are recommended. Several influencing parameters such as post type, luting material, core material, type of coronal restoration, have already been investigated [6]. Moreover the success of the adhesive restoration depends on a reasonable adhesion to the tooth substance and thus on the available bonding area. To evaluate the real impact of the available dentin surface on fracture resistance of restored teeth accurate and detailed measurements are mandatory.

One approach uses the CEREC system (Sirona Dental Systems, Bensheim, Germany) for acquiring an optical impression of the prepared tooth and for the calculation of the adhesive surface [7]. However the method is dependent on a well-defined coronal preparation without undercuts and is therefore less applicable for evaluation of geometric parameters in the root canal.

*hans.deyhle@unibas.ch; phone 41 61 265-9659; fax 41 61 265-9699; www.bmc.unibas.ch

The most reasonable approach for metric assessment of root canal volumes and surfaces is based on micro computed tomography (μCT) [8] since it provides reproducible data with micrometer precision irrespective of the complexity of the morphology involved [9].

The aim of the present investigation is to establish a standardized method for the detailed measurement of the bonding areas inside and outside of the post space and of the volume of the dowel space in severely compromised RCT teeth. The acquired morphological data can be correlated with mechanical parameters such as the fracture resistance after chewing-simulation. This approach seeks to identify suitable geometric parameters for predicting failures in restored RCT teeth and could be used in further in-vitro studies and to draw conclusions for the daily dental praxis.

2. MATERIALS AND METHODS

2.1 Tooth model

The investigation included 140 root-canal-treated human premolars prepared for post cementation as described in Figure 1. The first step was the decapitation of the tooth: 1 mm below the buccal cemento-enamel junction (CEJ) the clinical crowns were cut using a diamond bur, leaving a root length of (13 ± 1) mm. Subsequently, the roots were cleaned with scalers and dried with paper points. The second step was the filling of the root canal with gutta-percha (Obtura II, Obtura Corporation, Fenton, MO, USA) using an epoxy sealer (AH plus, Dentsply De Trey, Konstanz, Germany) to prevent intra-canal infections. During the third preparation step, the post space was generated with two types of pilot drills to obtain the desired form-congruence with the post applied (see below). The forth step is especially important for the present study. It was performed to quantity the important morphology parameters, i.e. the intra-radicular volume and the amputation area or the cross-section area of the decapitated tooth. A silicon impression material (President regular body, Coltene-Whaledent AG, Altstaetten, Switzerland) stabilized by a wooden toothpick served for the casting. These silicon impressions (see photograph in Figure 2) were characterized using μCT. After the removal of the silicone impressions, the posts were cemented as step 5 (see below). Finally, during processing step 6 artificial crowns were build-up to carry out realistic in-vitro tests of the mechanical properties. This step included the restoration of the coronal part of each tooth using composite crowns of the dual-curing resin luting material (Multicore Flow, Ivoclar Vivadent, Schaan, Lichtenstein). Despite the differences in the cervical root diameters, identical crowns 4 mm high were added using transparent molds (Pella crowns, Odus, Dietikon, Switzerland) with an anatomically shaped occlusal surfaces. The composite resin free of bubbles was filled into the mold and light-cured from the different sides for periods of 40 s. Excess composite resin in the cervical area was detached.

According to the dental treatments, which included different posts, the specimens were divided into six groups. The aim of the study was to determine the influence of post material, post length, and post fit (form congruence) on the mechanical stability of the restoration. Therefore, pilot drills with different apical diameters were used to intentionally realize different post fittings. The drills for the post space preparation of the Groups 1, 2, and 3 showed an identical apical diameter as the post to be inserted (form-congruence). Post and post space of the Groups 4 and 5 showed a 300 μm larger diameter along the entire post length (no form-congruence). In Group 6, no post was used. Here, the composite resin served as the intra-canal anchorage. Figure 3 summarizes the characteristics of the six groups, which includes the post material, the number of specimens per group and the scheme of the form-congruence.
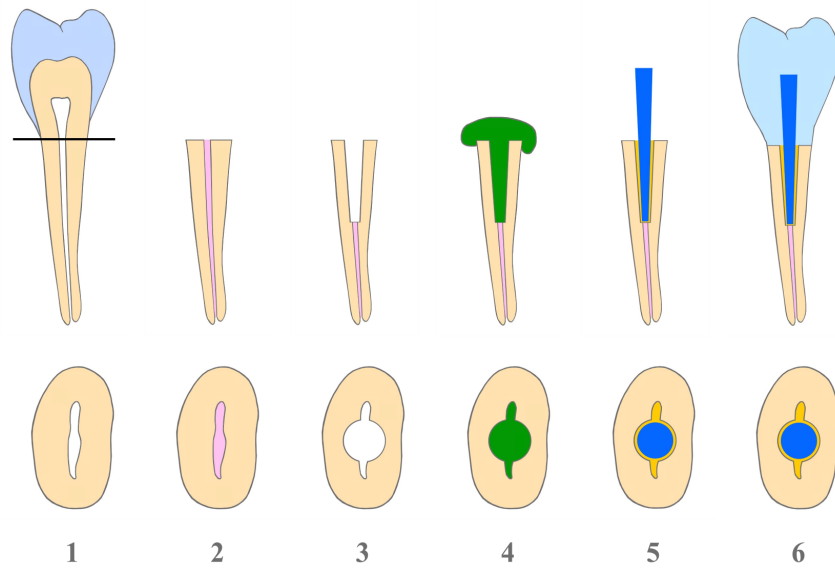
Figure 1. Preparation sequence: (1) Teeth were decapitated; (2) Root-canals were filled with gutta-percha; (3) The post space was prepared; (4) Impression taking was conducted; (5) Posts were adhesively cemented; (6) Direct composite crown build-ups were fabricated.
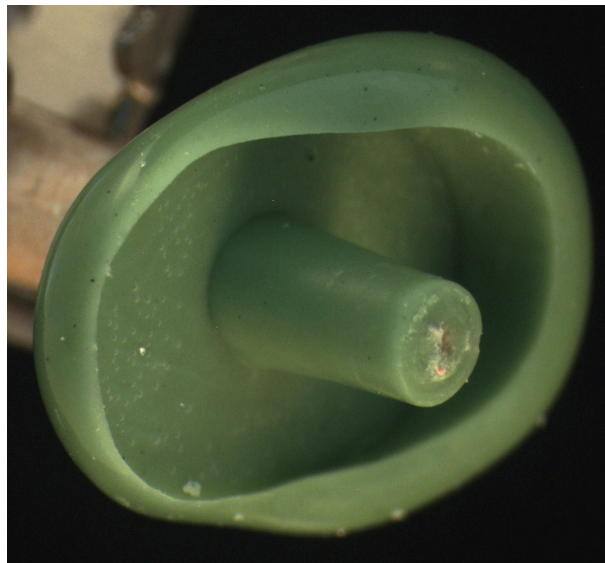

Figure 2. Silicone impression used to extract the morphological parameters of decapitated teeth by means of μCT data and sophisticated software tools.
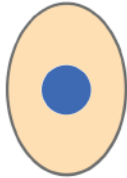
Figure 3. The different restoration treatments are schematically summarized together with the information on number of specimens per group as well as post materials and depth of post spaces.

2.2 Conventional μCT

Three-dimensional data of the silicone impressions were acquired with a SkyScan 1174™ system (SkyScan, Kontich, Belgium) with an acceleration voltage of 50 kV and a beam current of 800 μA. For each of the 137 specimens, 1,800 projections of 1024 × 1024 pixels equally distributed over 360° were recorded with an exposure time of 1.5 s per projection. The optical magnification was selected for a voxel length of 14.3 μm. The data were reconstructed with the supplier's software NRecon that is based on a modified Feldkamp algorithm. Both ring artifact and beam hardening corrections were applied.

2.3 Synchrotron radiation-based μCT

The synchrotron radiation-based μCT (SRμCT) experiment was performed at the beamline BW2 (HASYLAB at DESY, Hamburg, Germany) in standard absorption contrast mode. The tomography setup is operated by the GKSS Research Center [10]. Using a photon energy of 22 keV, 720 projections each 1536 × 1024 pixels were taken in equidistant angular steps between 0 and 180° in two height levels. The pixel size was set to 5.04 μm and resulted in the spatial resolution of 9.44 μm as determined from the 10% value of the modulated transfer function of a highly X-ray absorbing metal edge [11].

Before reconstruction, the projections were binned by a factor of two to reduce the data size and to increase the contrast [12]. The 3D dataset was reconstructed using a filtered back-projection algorithm available at beamline, resulting in a volume of 768 × 768 × 650 voxels.

2.4 Tomography data evaluation for the extraction of morphological parameters

The silicone impressions have to be segmented in order to extract the morphological characteristics of the decapitated teeth. For this purpose Image Lab GmbH, Winterthur, Switzerland developed the software package segm3D. It allows the semi-automatic segmentation of surface areas of the impression. An intensity-based segmentation tool allows differentiating between silicone and air in an automatic way similar to the approach described previously [13]. Subsequently, the operator can correct the result. It is, for example, necessary to exclude air inclusions (pores). The precise determination of surfaces from voxel-based data, however, is always complex and especially difficult for data with limited photon statistics. Therefore, the extraction of the morphological parameters is done in the following manner.

After the transformation of the tomography data into the .raw format, the centerline of the tooth root has been determined. Subsequently, the around 100 radial slices through the center of the root were created from the 3D datasets (see Figure 4). The outer edges of the amputation surface were marked manually in each radial slice. Subsequently, the edge line of amputation surface and root was determined automatically based on the contrast difference between silicone and air. The boundary between post and amputation surface was automatically found because of the changes in curvature, which only significantly increase at the transitions. The amputation surface characterized by the blue-colored line in Figure 4 is flat.

Unfortunately, the impressions contain a number of air inclusions especially at the periphery of the root, as shown in Figure 5. These defects can only be corrected manually. The software, however, is supportive allowing closing pores with a virtual pen.
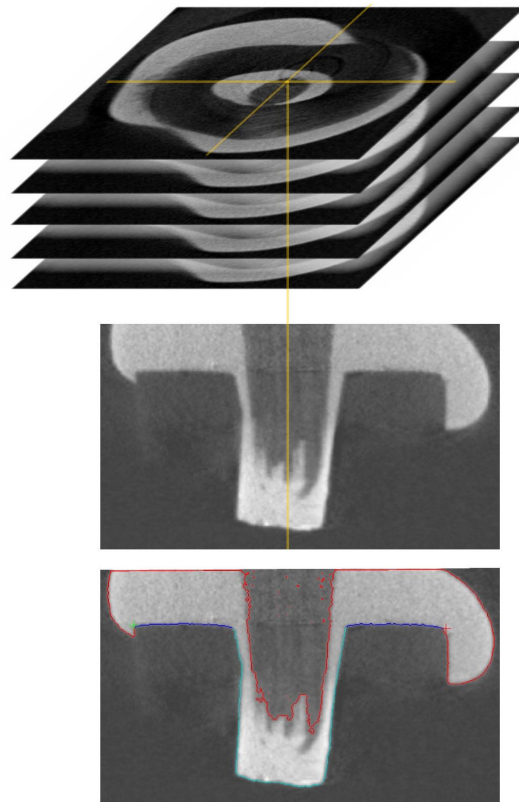

Figure 4. The images illustrate the determination of the tooth morphology from µCT-data of the silicone impression.
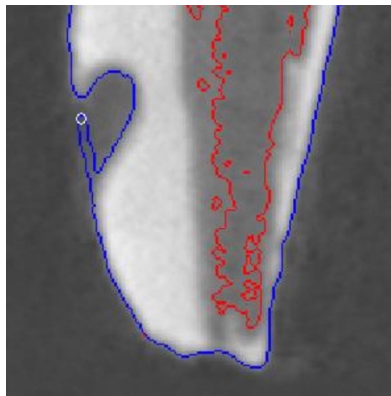
Figure 5. Marginal air bubbles in the impression material, as clearly identified on the left of the virtual cut, can be closed manually to correct the data.

The semi-automatically segmented interfaces are visualized for quantification by means of a mesh using the software MeshLab (Visual Computing Lab at the ISTI – CNR, http://meshlab.sourceforge.net). For noise reduction, established filters are incorporated with the aim to obtain a rather smooth interface.

The graphical representation of the mesh provides the operator with a visual feedback of the segmentation and serves for the calculation of the morphology of the decapitated teeth. This approach allows extracting the amputation area, the morphology of the root and the space for the post to be inserted.

2.5 Mechanical characterization

The roots of the teeth were coated with a 0.3 mm-thin polyvinylsiloxane layer (President light body, Colte`ne-Whaledent AG, Altstätten, Switzerland) to simulate a periodontal ligament. The specimens were glued with light-curing composite on the custom-made metallic holders (Provac, Balzers, Liechtenstein). The tooth roots were embedded in self-curing acrylic resin (Demotec 20, Demotec Siegfried Demel, Nidderau, Germany) about 1.5 mm above the simulated bone level. After this embedding, the specimens were stored in water until the mechanical testing should be performed. loading. To simulate the dynamic loading of human teeth, all specimens were mechanically loaded at the center of the occlusal surface with a force of 49 N for 1.2 million cycles using a frequency of 1.7 Hz by means of a computer-controlled masticator (CoCoM 2, PPK, Zürich, Switzerland) to simulate of a clinical service of five years. The specimen were simultaneously treated by 3,000 thermal changes between 5 and 50 °C to even better fit the clinical service of five years [14].

After the dynamic loading, where only about 5% of the specimens failed, the specimens were statically loaded until fracture using a universal testing machine (Zwick, Ulm, Germany). The specimens were fixed with the long axis of the roots at an angle of 45° as shown in Figure 6. A 0.5 mm-thin tin foil was positioned between steel sphere and artificial crown to prevent stress peaks. The compressive load was applied with constant speed of 0.5 mm per minute at the central fissure of the occlusal surface in direction of the buccal cusp until failure. A characteristic stress-strain curve is represented in Figure 6. It allows for the determination of the effective Young's modulus E and the maximal load F_{max}.
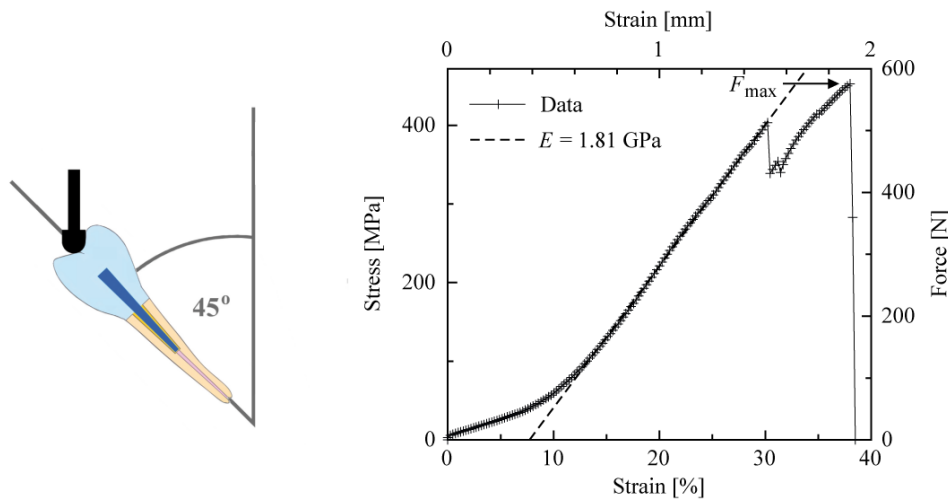

Figure 6. The scheme on the left shows the test geometry for the compressive loading. The diagram on the right – a characteristic stress-strain curve of the entire experimental setup – shows how the Young's modulus E and the maximal load F_{max} were determined. The Young's modulus corresponds to the maximal slope present within a significant strain range as indicated by the dashed line.

3. RESULTS

Figure 7 shows the direct comparison between the conventional SkyScan μCT and the SRμCT data. Although more details are seen on the SRμCT image, the amputation interface, which is olive green colored, and the root of the tooth prepared for the post insertion, which is pink colored, are also well reproduced from the conventional approach. Because of the better accessibility of the conventional source, the silicone impressions are measured with the SkyScan system here. Note, the 3D data were rigidly registered using the algorithm described by Fierz et al. [15] to prove the statement.
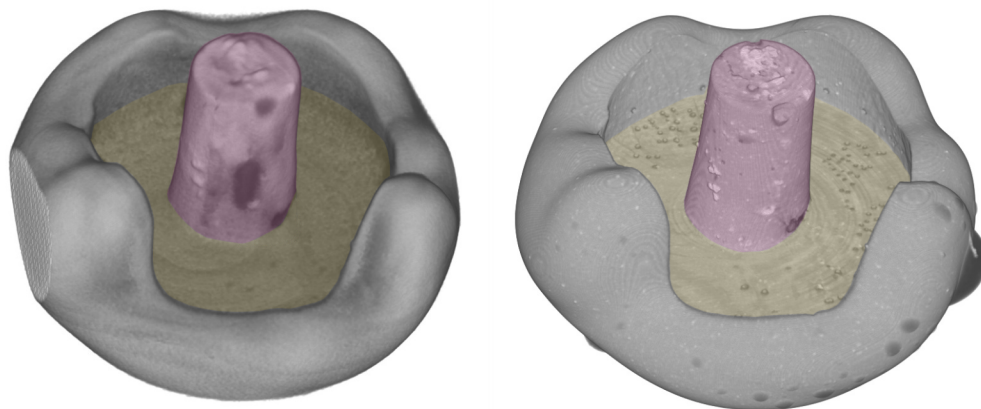
Figure 7. The comparison between conventional and SRµCT is qualitatively demonstrated by two 3D representations of registered datasets.

The morphological and mechanical data are summarized for the different groups in Table 1. The error bars correspond to the standard deviations.

The Young's modulus does not show significant differences between the groups. Using the Tukey-Kramer test one finds that the fracture resistance given by the maximal load is significantly higher in Groups 2 and 4 compared to the specimens of the other groups.

The morphological data show significant differences for Group 4 with respect to the amputation surface and the root canal volume compared to the other groups.

The amputation interface is the parameter that best differentiates between the six groups.

Table 1. Mean values and standard deviations of the mechanical and geometrical parameters.

Group	Young's modulus E [GPa]	Maximal load F_{max} [N]	Amputation interface [mm^2]	Root canal surface [mm^2]	Root canal volume [mm^3]
1	1.41 ± 0.32	295 ± 82	28 ± 4	24 ± 7	91 ± 25
2	1.97 ± 0.36	394 ± 99	27 ± 7	24 ± 5	84 ± 30
3	1.64 ± 0.49	275 ± 76	18 ± 3	20 ± 4	56 ± 12
4	1.68 ± 0.38	408 ± 131	42 ± 12	25 ± 9	173 ± 74
5	1.53 ± 0.33	237 ± 97	21 ± 5	22 ± 5	84 ± 27
6	1.70 ± 0.44	253 ± 71	23 ± 6	25 ± 7	81 ± 24

One may assume a clear difference between the two depths of the intra-radicular anchorage of 3 mm and 6 mm, respectively. Therefore, these two situations were averaged and presented in Table 2. This means that the Groups 1, 2, and 4 as well as the Groups 3, 5, and 6 were combined. The values given in Table 2, however, do not allow differentiating between the values for the different post lengths introduced, although the Tukey-Kramer test does.

Table 2. Mean values of the mechanical and geometrical parameters for 3 mm and 6 mm-long incorporated posts.

Post length	Young's modulus E [GPa]	Maximal load F_{max} [N]	Amputation interface [mm^2]	Post canal surface [mm^2]	Post canal volume [mm^3]
3 mm	1.6 ± 0.5	260 ± 89	20 ± 4	21 ± 4	69 ± 23
6 mm	1.8 ± 0.4	404 ± 113	34 ± 11	24 ± 7	125 ± 64

The mechanical tests are to be detailed correlated with the morphological data. Therefore, the Young's modulus and the maximal loads were plotted against the amputation interface for the different groups in Figure 8 and for the different post lengths in the tooth roots in Figure 9. They demonstrate a biased selection of the teeth. While the Young's modulus remains more or less constant for teeth of different sizes, the ultimate compressive strength of the constructs seem to scale with the amputation interface in more or less linear fashion.
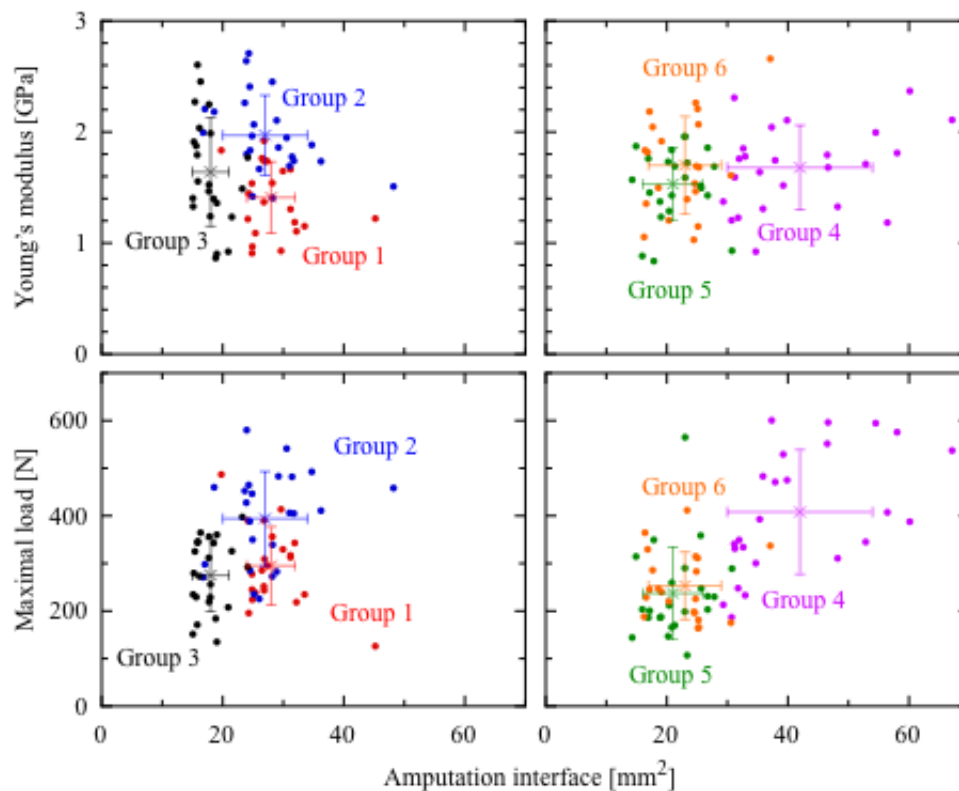

Figure 8. The Young's modulus is more or less constant for the six groups, whereas the maximal load seems to depend on the amputation interface in linear fashion.
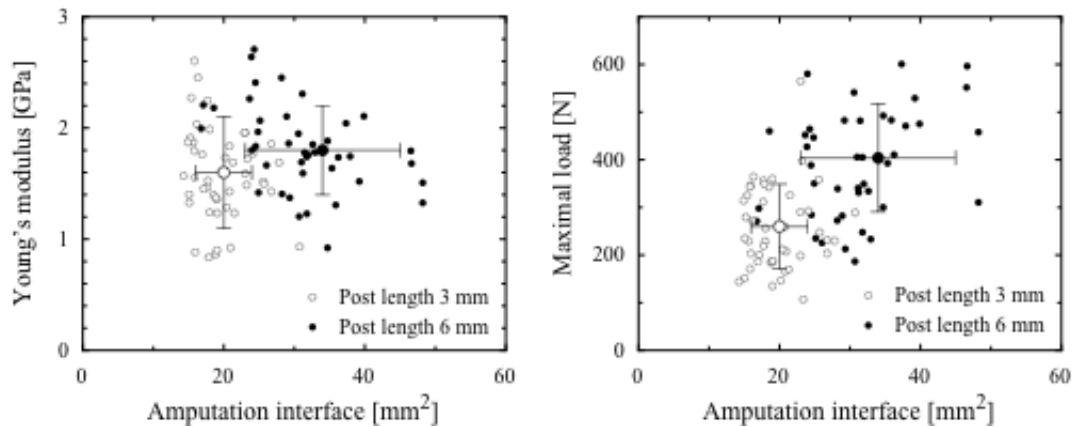
Figure 9. Larger teeth are selected to place the longer posts. Therefore, especially the maximal load seems to depend on the post length.

4. DISCUSSION

In-vitro laboratory tests with restored human root canal treated teeth aim to predict the clinical performance. This is, however, challenging since such investigations only partially reflect the clinical situation and, even more important, testing human teeth leads to considerable standard deviations [14].

The effective Young's modulus determined in the present study does not depend on the morphological parameters, which indicates the sound reproducibility of the individual mechanical characteristics of the specimens. Its mean value corresponds to 1.7 GPa, but still exhibits significant scattering. Therefore, the number of 24 specimens per group becomes reasonable. This effective Young's modulus is too low to be comparable to established data of dentin (E_{dentin} = 20 GPa [16]). Thus the values resulting from the area of elastic deformation in the stress/strain plots are most likely attributed to the composite material used for both build-up and post cementation. The value specified by the manufacturer is also higher (7 GPa), but the physical properties of resin-based materials are known to be significantly affected by water storage [17] as performed during the thermo-cycling process. Because the effective Young's modulus characterizes the weakest part of the set-up or the combination of the weaker components the quantity derived is understandable.

As demonstrated earlier [18], the fracture resistance is influenced by the insertion depth of the post since both mechanical retention and adhesive surface increase when 6 mm-long posts compared to 3 mm-long posts are incorporated. This is revealed by the μCT data of the root canal surface although the difference was not statistically significant. On the contrary a form-congruence between post and root canal seems to be of minor importance. These findings suggest that a perfectly fitting post is not necessarily required. Among the morphological parameters tested the surface in the root canal had the greatest impact on fracture resistance even when only specimens of the 6 mm insertion depth were analyzed.

It is surprising that the Group 6 specimens exhibit a fracture resistance in the range of the other groups, because no post was applied. For the clinical pratice, one has to note, however, that the thermo-cyclic dynamic testing and the handling faults resulted in three failures out of 24 specimens, whereas for the Postec-specimens only maximal one failed (cp. Figure 3). Therefore, one may state, that there is much less influence of post material on the mechanical performance during the in-vitro tests than originally expected.

The evaluation of the tooth morphology using micro computed tomography and sophisticated data treatments uncovered the biased choice of teeth for the different groups. The amputation interface was by trend almost a factor of two larger for the 6 mm post insertion lengths compared to the 3 mm insertion lengths. For Group 4 the amputation interface was significantly larger – by a factor of two - than for the Groups 5 and 6. Obviously even though it was attempted to choose teeth with similar dimensions at the cemento-enamel junction and to equally allocate them to the experimental groups like done in the investigation of Büttel et al. [18], this approach does not guarantee a non-biased distribution of the

specimens. Against this background one might hypothesize that the significant differences found are merely the result of an unequal distribution. The statistical analysis considering only teeth with a similar size in terms of the calculated amputation interface, however, does not support the assumption for the data presented.

Nevertheless, the proposed μCT examination should have been performed before post insertion to guarantee a well-distributed choice of teeth. This approach allows conducting in-vitro studies with a higher accuracy and can be recommended for further laboratory investigations where the morphology of human teeth may influence the results.

5. CONCLUSION

The combination of μCT and appropriate software for 3D data evaluation enables us to get a detailed insight into the quantitative morphological characterization of treated teeth. The present study also elucidates that conventional μCT provides already reasonable morphological results and one can abstain from the expensive synchrotron radiation-based measurements for the rather large number of individual specimens.

REFERENCES

[1]   V. G. Clavijo, J. M. Reis, W. Kabbach *et al.*, "Fracture strength of flared bovine roots restored with different intraradicular posts," J Appl Oral Sci, 17(6), 574-8 (2009).

[2]   R. S. Schwartz, and J. W. Robbins, "Post placement and restoration of endodontically treated teeth: a literature review," J.Endod., 30(5), 289-301 (2004).

[3]   W. M. Fennis, R. H. Kuijs, C. M. Kreulen *et al.*, "A survey of cusp fractures in a population of general dental practices," Int J Prosthodont, 15(6), 559-563 (2002).

[4]   N. Fritz, M. Illert, S. de la Motte *et al.*, "Pattern of monosynaptic Ia connections in the cat forelimb," J Physiol, 419, 321-51 (1989).

[5]   H. Lang, Y. Korkmaz, K. Schneider *et al.*, "Impact of endodontic treatments on the rigidity of the root," J.Dent.Res., 85(4), 364-368 (2006).

[6]   K. Bitter, and A. M. Kielbassa, "Post-endodontic restorations with adhesively luted fiber-reinforced composite post systems: a review," Am J Dent, 20(6), 353-60 (2007).

[7]   W. H. Mormann, and A. Bindl, "The bonding area of intra- and extra-coronal tooth preparations," Am J Dent, 19(4), 201-5 (2006).

[8]   O. A. Peters, A. Laib, P. Ruegsegger *et al.*, "Three-dimensional analysis of root canal geometry by high-resolution computed tomography," J Dent Res, 79(6), 1405-9 (2000).

[9]   J. S. Rhodes, T. R. Ford, J. A. Lynch *et al.*, "Micro-computed tomography: a new tool for experimental endodontology," Int Endod J, 32(3), 165-70 (1999).

[10] F. Beckmann, "Microtomography using synchrotron radiation as a user experiment at beamlines BW2 and BW5 of HASYLAB at DESY," Proc. SPIE. 4503, 34-41 (2002)

[11] B. Müller, P. Thurner, F. Beckmann *et al.*, "Non-destructive three-dimensional evaluation of biocompatible materials by microtomography using synchrotron radiation," Proc. SPIE. 4503, 178-188 (2002)

[12] P. Thurner, F. Beckmann, and B. Müller, "An optimization procedure for spatial and density resolution in hard X-ray micro-computed tomography," Nucl. Instrum. Meth., 225(4), 599-603 (2004).

[13] B. Müller, F. Beckmann, M. Huser *et al.*, "Non-destructive three-dimensional evaluation of a polymer sponge by micro-tomography using synchrotron radiation " Biomolecular Engineering, 19, 73-78 (2002).

[14] I. Krejci, E. Mueller, and F. Lutz, "Effects of Thermocycling and Occlusal Force on Adhesive Composite Crowns," Journal of Dental Research, 73(6), 1228-1232 (1994).

[15] F. C. Fierz, F. Beckmann, M. Huser *et al.*, "The morphology of anisotropic 3D-printed hydroxyapatite scaffolds," Biomaterials, 29, 3799-3806 (2008).

[16] V. Imbeni, J. J. Kruzic, G. W. Marshall *et al.*, "The dentin-enamel junction and the fracture of human teeth," Nature Materials, 4(3), 229-232 (2005).

[17] H. Oysaed, and I. E. Ruyter, "Composites for use in posterior teeth: mechanical properties tested under dry and wet conditions," J Biomed Mater Res, 20(2), 261-71 (1986).

[18] L. Buttel, G. Krastl, H. Lorch *et al.*, "Influence of post fit and post length on fracture resistance," Int Endod J, 42(1), 47-53 (2009).